International Journal of Science, Strategic Management and Technology
Volume **02** Issue **11** November-2026 | ISSN: **3108-1762 (Online)** | Impact Factor: 3.8
An International, Peer-Reviewed, Open Access Scholarly Journal Indexed in recognized academic databases

Analyzing Printability Layer Bond Strength and Material Mix Design for Automated Concrete Construction

ASHUTOSH LUHANIA
Assistant Professor, Department of Civil Engineering
Jagannath University, Jaipur, Rajasthan, India

https://doi.org/10.55041/ijsmt.v2i11.026

Cite this Article: LUHANIA, A. (2026). Analyzing Printability Layer Bond Strength and Material Mix Design for Automated Concrete Construction. International Journal of Science, Strategic Management and Technology, *02*(11), 1-9. https://doi.org/10.55041/ijsmt.v2i11.026

License: This article is published under the Creative Commons Attribution 4.0 International License (CC BY 4.0), permitting use, distribution, and reproduction in any medium, provided the original author(s) and source are properly credited.

Abstract—Extrusion-based three-dimensional concrete printing replaces formwork with a digitally controlled material-process system, but the same layer-wise operation creates a narrow operating window between pumpability, extrudability, buildability, open time, and interlayer adhesion. This paper integrates mixture proportioning, fresh-state mechanics, process parameters, and hardened interface performance into a single qualification framework for automated concrete construction. Two transparent literature datasets are re-analyzed: the five-mixture high-performance printable concrete series reported by Le et al., and the 192-test TU/e program reported by Wolfs et al. The latter shows that, under protected interfaces, flexural tensile strength normal to the layer plane decreased from 3.68 MPa at a 15 s interval to 3.10 MPa at 24 h, while splitting tensile strength decreased from 3.55 to 2.80 MPa. At a 4 h interval, leaving the surface uncovered reduced flexural tensile strength from 3.48 to 1.72 MPa, demonstrating that elapsed time alone is an incomplete control variable; moisture state and structural build-up must be monitored concurrently. A performance-based mix-design procedure is proposed using particle packing, water-to-binder ratio, rheology modifiers, supplementary cementitious materials, fibers, and staged admixture dosing. The resulting quality plan combines ram/extrusion testing, yield-stress evolution, dimensional stability, interface moisture, and bond tests with in-process sensing. The paper concludes that reliable automated construction requires qualification of the complete material-machine-environment combination rather than approval of a mix in isolation.

Index Terms—3D concrete printing, additive manufacturing, automated construction, buildability, extrudability, interlayer bond, mix design, printability, rheology, structural build-up.

I. INTRODUCTION

Automated concrete construction links a digital model to mixing, pumping, robotic motion, and layer-by-layer deposition. Removing formwork can reduce geometric constraints and material waste, yet it also transfers quality control from a passive mould to a time-dependent material-process interaction. A printable cementitious material must move through the pump and nozzle without segregation, emerge as a continuous filament, retain the intended cross-section, carry the weight of later layers, and form interfaces that remain mechanically reliable. These requirements compete: a fluid mixture is easy to pump but prone to deformation, while a rapidly structuring mixture carries layers well but may clog the delivery line and bond poorly after a delay [1]–[5].

The central engineering problem is therefore not a single target strength. It is the identification and maintenance of a process window. Within that window, fresh-state yield stress is low enough under shearing for transport and extrusion, high enough after deposition for shape stability, and recoverable at a controlled rate. The open time must cover the planned print duration, while the interlayer interval must not permit excessive drying or surface stiffening. The deposited bead geometry must be consistent with the toolpath so that the intended wall thickness, void ratio, and load path are actually manufactured.

Interlayer interfaces are structurally important because their properties are created during fabrication. Time gap, ambient temperature, relative humidity, air movement, nozzle stand-off, deposition pressure, substrate deformation, and surface moisture interact with mixture chemistry. A nominally identical material can consequently produce distinct bond strengths on different machines or under different site conditions. This explains why published studies sometimes report markedly different losses for apparently similar time gaps [5]–[9].

This paper provides an integrated analysis suited to research and engineering qualification. It synthesizes established rheological models and test methods, reproduces published mixture and bond-strength datasets, derives normalized indicators, and proposes a practical control plan. It does not claim a new laboratory campaign. Numerical results identified as secondary analysis were calculated from values reported in the cited experimental studies. This distinction supports reproducibility and prevents literature-derived observations from being mistaken for original measurements.

The main contribution is a traceable chain connecting mixture constituents to fresh-state response, print parameters, interface condition, and hardened performance. The framework is intended for gantry or robotic-arm extrusion systems using fine-aggregate concrete or mortar. It is applicable to factory and site printing, but project-specific validation remains necessary whenever the binder, aggregate grading, pump-hose system, nozzle, layer geometry, reinforcement concept, or environmental exposure changes.

© Author(s). This work is peer-reviewed, openly published, and permanently archived
This article is openly accessible and reusable with proper attribution.

International Journal of Science, Strategic Management and Technology
Volume 02 Issue 11 November-2026 | ISSN: 3108-1762 (Online) | Impact Factor: 3.8
An International, Peer-Reviewed, Open Access Scholarly Journal Indexed in recognized academic databases

II. RESEARCH QUESTIONS AND CONTRIBUTION

The study addresses four questions. First, which measurable properties define printability without collapsing it into a subjective visual judgment? Second, how do mixture proportions and admixtures move the material through the pumpability-buildability trade-off? Third, which process variables dominate interlayer bond strength, and how should published bond data be interpreted? Fourth, what qualification and in-process acceptance system can convert laboratory knowledge into repeatable automated construction?

The analysis treats printability as a vector rather than a binary label. The vector contains pump pressure stability, extrudability, filament continuity, width and height retention, structural build-up rate, open time, and layer-to-layer conformity. A material is accepted only when every critical component lies within the machine- and geometry-specific limits. This avoids the common failure in which a mixture passes an extrusion trial but deforms in a tall wall, or prints a stable wall but produces a weak cold joint after an interruption.

A second contribution is the separation of intrinsic material variables from state variables. Binder chemistry, particle-size distribution, fiber content, and admixture dosage define potential behavior. Temperature, resting time, shear history, moisture loss, and pressure history define the state at the instant of deposition. The latter variables can change within one batch; they must therefore be sensed or bounded during production instead of being assumed constant from the batch ticket.

The paper also uses dimensionless ratios wherever possible. Examples include actual-to-commanded volumetric flow, bead width-to-nozzle width, layer height-to-nozzle stand-off, bond-to-matrix tensile strength, and deposited stress-to-fresh yield capacity. Dimensionless reporting improves comparison between printers of different scale and makes acceptance logic portable, provided that raw dimensions and test conditions are retained.

Finally, the proposed framework distinguishes qualification, pre-production verification, and production control. Qualification establishes the viable material-machine-environment envelope. Pre-production verification confirms that current materials and equipment reproduce the qualified state. Production control detects drift in real time and defines stop, correct, requalify, and document decisions. This layered approach is more defensible than relying on 28-day strength after the printed member has already been manufactured.

III. AUTOMATED CONCRETE PRINTING SYSTEM

An extrusion printing system includes storage and batching, a high-shear or continuous mixer, a pump, delivery hose, print head, nozzle, motion platform, control software, and sensors. The material experiences multiple shear regimes: mixing disperses agglomerates; pumping breaks down thixotropic structure; hose residence allows partial rebuilding; nozzle contraction increases shear; and deposition removes most imposed shear. The final bead response is therefore path-dependent. A laboratory test performed on material that did not experience the production shear history may overestimate yield stress or underestimate pumping demand.

The commanded tool speed and material flow must be synchronized. For a rectangular idealized bead of width b and height h, conservation of volume gives Q = b h v, where Q is volumetric flow and v is nozzle travel speed. Real beads have rounded shoulders and may contain voids, so a shape factor is required. If Q/v is too low, adjacent filaments separate or neck; if too high, the bead bulges, the nozzle ploughs the material, or the layer width exceeds the digital model. Closed-loop control should therefore compare observed cross-sectional area with Q/v rather than monitor pump speed alone.



Fig. 1. Coupled material-process-property chain for extrusion-based automated concrete construction.

Layer height is commonly selected below the unconstrained nozzle dimension to impose mild compression and promote contact. Excessive stand-off reduces compaction and can create a rounded, weakly contacting interface. Excessive squeeze can cause lateral flow, tool collision, and geometric error. The optimum depends on aggregate size, bead aspect ratio, yield stress, extrusion pressure, and the capacity of the lower layer at its current age.

Print-path planning influences both fresh stability and bond. Long contours increase the interval before a nozzle returns to the same location. Corners introduce deceleration and locally excessive deposition unless flow is adjusted. Starts and stops create discontinuities, while crossovers can cause geometric and moisture irregularities. A structural toolpath should be reviewed as a construction sequence, not only as a geometric slicing output.

Environmental control is part of the system. Direct sun, low relative humidity, hot substrates, and air movement can desiccate a layer within the nominal open time. Conversely, rain, misting, or excessive interface water can reduce friction and produce a lubricated plane. Enclosures, wind shields, substrate conditioning, temperature logging, and controlled curing are process equipment for structural reliability, not optional site conveniences.

IV. DEFINING AND MEASURING PRINTABILITY

Pumpability is the ability to transport a homogeneous mixture at the required flow without excessive pressure, blockage, bleeding, or segregation. It is assessed using pressure-flow response, pump power, hose temperature, and discharged uniformity. A stable pressure trace is as important as the mean pressure because oscillation can produce cyclic bead-width errors. Scale matters: a bench syringe cannot reproduce plug flow, wall slip, aggregate migration, or pressure loss in a long production hose.

Extrudability is the ability to pass through the nozzle as a continuous filament with acceptable surface quality. A practical test records the minimum stable flow, maximum stable flow, extrusion pressure, occurrence of tearing, and mass per unit length. Visual continuity should be supplemented by image-based width and edge-roughness measurements. A pass criterion may require no blockage, no visible segregation, and a coefficient of variation in bead width below a project-defined threshold over a representative travel length.

Buildability is the capacity of deposited layers to preserve geometry and resist buckling, plastic collapse, or excessive settlement during construction. Layer count alone is not a

© Author(s). This work is peer-reviewed, openly published, and permanently archived
This article is openly accessible and reusable with proper attribution.

International Journal of Science, Strategic Management and Technology
Volume **02** Issue **11** November-2026 | ISSN: **3108-1762 (Online)** | Impact Factor: 3.8
An International, Peer-Reviewed, Open Access Scholarly Journal Indexed in recognized academic databases

transferable measure because it depends on bead dimensions, print speed, contour length, and waiting time. Better metrics include vertical strain after a specified stress history, maximum stable height under a defined deposition schedule, and the evolution of static yield stress or green strength.

TABLE I. PERFORMANCE-BASED PRINTABILITY ATTRIBUTES

Attribute	Primary metric	Typical failure signal
Pumpability	Pressure-flow stability	Pressure drift, segregation, blockage
Extrudability	Continuous bead and mass/length	Tearing, pulsation, discontinuity
Buildability	Stable height and vertical strain	Settlement, lean, buckling
Open time	Time to first failed criterion	Pressure, geometry, or bond limit
Accuracy	Width, height, path deviation	Bias or high local variation

Open time is the period during which the material remains within every required fresh-property limit. It should be measured under the actual storage and recirculation protocol. An extrusion-only open time may be dangerously optimistic if the later material still exits the nozzle but has lost interface wetting or produces a rough bead. The end of open time is the earliest failure among pressure, continuity, geometry, buildability, and bond-related criteria.

Print quality combines dimensional accuracy, surface condition, internal voids, and interface conformity. Useful geometric indices are width error $e_b=(b_m-b_t)/b_t$, height error $e_h=(h_m-h_t)/h_t$, and area-delivery error $e_A=(A_m-Q/v)/(Q/v)$. These are calculated for local and moving-average windows so that short transient defects and sustained drift are both detected. Laser profiles, structured-light cameras, or stereo vision can automate these measurements.

No single test fully predicts printing performance. A robust qualification matrix includes a rheometer or vane test, a pumping loop, a nozzle extrusion test, a multi-layer build test, and a hardened interface test. The scale and sequence should progressively approach production conditions. The material passes only if its performance remains acceptable after the same rest, remixing, pumping, hose, and deposition history planned for the project.

V. FRESH STATE MECHANICS AND FAILURE MODELS

Fresh printable concrete is often approximated as a yield-stress fluid. The Bingham relation $\tau=\tau_0+\mu\dot{\gamma}$ describes shear stress τ above yield as the sum of yield stress τ_0 and plastic-viscosity term $\mu\dot{\gamma}$. The Herschel-Bulkley model adds an exponent n and better represents shear thinning. These idealizations are useful for comparing mixtures, but wall slip, granular friction, thixotropy, and localization can dominate in pumps and nozzles. The test geometry, shear protocol, elapsed time, and pre-shear must accompany every reported rheological value.

Structural build-up describes the recovery and growth of resistance at rest. A linear early-age approximation writes $\tau_0(t)=\tau_{0,0}+A_{thix}\,t$, where A_{thix} is the structuration rate. The approximation should only be used within the measured interval because hydration can accelerate the response. Build-up supports later layers, but a high rate also reduces interface remobilization. The desired value is consequently determined by the planned layer cycle and wall geometry, not maximized in isolation.

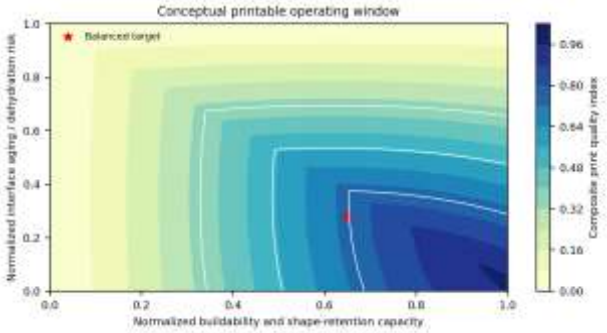


Fig. 3. Conceptual operating window showing that buildability must increase without excessive interface aging.

A lower-layer stress check compares gravitational demand with evolving green strength. For a straight wall of height H and density ρ, the average vertical stress near the base is approximately $\rho g H$, before geometric stress concentrations are included. Plastic yielding becomes possible when the relevant compressive or shear capacity is exceeded. Slender walls may buckle at lower stress, requiring a time-dependent stiffness and geometric-imperfection model. Overhangs introduce eccentricity and localized shear.

Interface formation includes wetting, mechanical interlocking, particle rearrangement, capillary exchange, and ongoing hydration across the contact. A newly deposited bead may remobilize the top of the earlier layer if surface moisture and deformability remain adequate. With time, evaporation and structural build-up reduce this mixing. The resulting interface can contain aligned pores, a distinct hydration zone, and preferential cracks. Micro-computed tomography and microscopy have demonstrated that extrusion can organize defects rather than distribute them randomly [10], [11].

These mechanisms explain the central process conflict. Rapid printing reduces interface aging but increases the rate of vertical load accumulation. Slow printing allows the base to strengthen but raises the risk of a dry or rigid surface. The optimum schedule is the fastest rate that does not violate fresh stability, with pauses controlled by moisture protection or deliberate interface treatment. A schedule must be evaluated locally because return time varies along complex toolpaths.

VI. MATERIAL MIX DESIGN

Printable mixtures are usually fine-aggregate concretes or mortars with a high powder fraction, controlled water content, and chemical admixtures. The fine grading reduces blockage risk and permits small nozzles, but high paste volume increases shrinkage, heat, embodied carbon, and cost. A rational design begins with the maximum aggregate size compatible with the smallest passage and hose, then maximizes well-graded aggregate within pumping and surface-quality limits. The remaining paste must lubricate transport, bind particles, and develop the required thixotropic recovery.

Portland cement supplies early hydration and strength. Fly ash can improve workability and reduce clinker content but may slow early build-up. Silica fume increases cohesion and particle packing, although excessive dosage increases water demand and pumping pressure. Limestone filler can tune grading and yield stress with lower reactivity. Slag, calcined clay, and other supplementary materials require characterization of setting and admixture compatibility. Replacement percentage alone is insufficient; surface area and packing control water and superplasticizer demand.

© Author(s). This work is peer-reviewed, openly published, and permanently archived
This article is openly accessible and reusable with proper attribution.

International Journal of Science, Strategic Management and Technology
Volume 02 Issue 11 November-2026 | ISSN: 3108-1762 (Online) | Impact Factor: 3.8
An International, Peer-Reviewed, Open Access Scholarly Journal Indexed in recognized academic databases

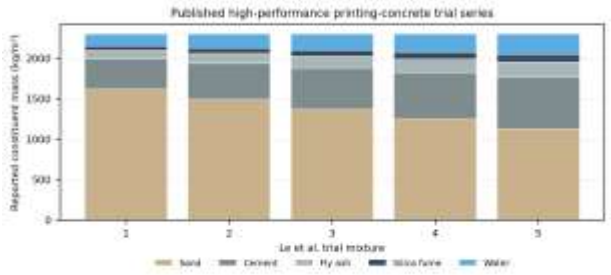


Fig. 2. Original re-plot of the five trial mixture proportions reported by Le et al. [1]. Minor admixtures and fibers are not shown.

Water-to-binder ratio affects strength, viscosity, bleeding, hydration, and open time. Lowering it generally improves shape retention but can sharply increase pressure unless a compatible high-range water reducer is used. Superplasticizer is therefore a process-control ingredient, not simply a strength aid. Viscosity-modifying agents and nanoclays can reduce segregation and accelerate structural recovery. Retarder protects open time, while accelerator may be dosed near the nozzle to decouple pumping from buildability. Such two-stage dosing needs mixing-energy verification and safeguards against local over-dosing.

Short fibers can control plastic cracking and improve post-cracking response. Their orientation is influenced by nozzle flow, which produces anisotropy. Fibers also increase pumping resistance and blockage risk, especially when length approaches nozzle dimensions or agglomeration occurs. Fiber type, aspect ratio, volume, dispersion procedure, and orientation relative to structural demand must be qualified together.

The published Le et al. trial series demonstrates systematic variation rather than a universal recipe [1]. Across Mixes 1–5, sand decreases while cement, fly ash, silica fume, and water increase. Mix 4, widely reproduced in later literature, contains 579 kg/m³ cement, 165 kg/m³ fly ash, 83 kg/m³ silica fume, 1241 kg/m³ sand, and 232 kg/m³ water before minor chemical admixtures and fibers. Its nominal water-to-total-binder ratio is 0.281. These values are a historical high-performance benchmark, not a sustainability optimum or direct site prescription.

TABLE II. LE ET AL. TRIAL MIXTURE SERIES IN kg/m³ [1]

Mix	Sand	Cement	Fly ash	Silica fume	Water
1	1612	376	107	54	150
2	1485	446	127	64	178
3	1362	513	147	73	205
4	1241	579	165	83	232
5	1123	643	184	92	257

A performance-based procedure uses iterative gates: particle packing and blockage screening; paste-volume and water-demand calculation; rheological screening after production-equivalent shear; pump-loop verification; extrusion and dimensional testing; multi-layer stability; open-time assessment; and hardened anisotropy and interface testing. A change in cement source, sand moisture, grading, admixture lot, hose length, or temperature can move the operating window and should trigger defined verification.

VII. INTERLAYER BOND MECHANISMS AND TESTING

Interlayer bond is governed by the weakest combination of interface area, defects, moisture condition, chemical continuity, and mechanical interlocking. A long time gap is a risk indicator, not a complete predictor. Two surfaces with the same delay can have different bond because one was covered and remained deformable while the other dried. Conversely, a very wet treatment may introduce a high-water plane. Interface condition should be recorded immediately before deposition using at least temperature, elapsed time, and a repeatable moisture or evaporation indicator.

Direct tension most directly represents opening normal to the layer plane, but specimen alignment and gripping are difficult. Splitting tension is easier yet creates a nonuniform stress field and depends on interface position. Flexural tests are practical and sensitive to a weak interface, but the calculated modulus of rupture is not a uniform direct tensile stress. Shear tests address sliding and roughness, while compression may hide a weak interface unless load direction or confinement activates it. Reported values from different test types should not be pooled without a conversion model.

Specimen extraction affects results. Sawing can damage edges, change the stressed area, or exclude the as-printed surface. Loading faces should be prepared without erasing the interface. The number of layers, interface location, dimensions, curing, age, loading rate, and failure path must be reported. A nominal strength value is incomplete if failures occurred outside the interface or if the bonded area was smaller than the gross area because of voids.

A useful normalized indicator is the bond efficiency $\eta_b = f_{interface}/f_{matrix}$, where f_{matrix} is measured with the same test configuration in material without a critical interface. This separates interface loss from batch strength. It should be presented with mean, standard deviation, sample count, and failure mode. Characteristic design values require a statistically justified population and account for production variability, not only carefully prepared laboratory specimens.

Interface treatment options include reducing the return time, protecting the surface, controlled misting, brushing or texturing, applying a compatible cementitious bonding layer, mechanically interlocking bead geometry, or locally remixing the surface. Each treatment can alter geometry, durability, or production rate. Qualification must verify not only immediate tensile strength but also shrinkage compatibility, permeability, freeze-thaw or chloride exposure where relevant, and repeatability under robotic timing.

VIII. DATA SOURCES AND SECONDARY ANALYSIS METHOD

The quantitative analysis uses two published sources selected because their procedures and numerical data are sufficiently transparent. The first is the five-trial mixture series of Le et al. [1], which progressed from aggregate-rich to powder-rich formulations and identified a printable high-performance mixture through laboratory tests and a full-scale bench demonstration. Constituent masses were digitized from the published table and checked against later reproductions. Minor admixture and fiber dosages are discussed qualitatively where the accessible tabulation is incomplete.

The second source is the TU/e program by Wolfs, Bos, and Salet [5]. A custom mortar was printed as 50 mm wide and 9.5 mm high layers using a gantry system, one-inch hose, and mixer-pump. The water-to-fines ratio was 0.495. Interlayer intervals of 15 s, 1 h, 4 h, 7 h, and 24 h; nozzle heights of 8.0, 9.5, and 11 mm; covered and uncovered surfaces; and three loading directions were evaluated. Seven specimens were used per series and 192 tests were reported. Samples were stored

© Author(s). This work is peer-reviewed, openly published, and permanently archived
This article is openly accessible and reusable with proper attribution.

International Journal of Science, Strategic Management and Technology
Volume **02** Issue **11** November-2026 | ISSN: **3108-1762 (Online)** | Impact Factor: 3.8
An International, Peer-Reviewed, Open Access Scholarly Journal Indexed in recognized academic databases

under plastic for 24 h, cut, water cured, and tested at seven days [5].

Reported means and standard deviations were entered without alteration. Percentage retention was calculated as 100 f_t/f_15s for each test method. The dehydration penalty was calculated as 100(1-f_uncovered/f_covered) at the same interval and nominal nozzle height. These calculations are descriptive and do not imply causality outside the tested material-process system. No synthetic replicate values were generated, and no inferential p-values were assigned where raw observations were unavailable.

TABLE III. TU/e FACTOR MATRIX SUMMARIZED FROM [5]

Study block	Levels	Response
Interlayer interval	15 s, 1, 4, 7, 24 h	Flexural or splitting tension
Nozzle height	8.0, 9.5, 11 mm	Flexural tension
Surface state	Covered, uncovered	Flexural tension
Direction	I, II, III	Flexure, splitting, compression

Figures in this paper are original visualizations of cited numerical data or original engineering schematics. They are not copied images from the source articles. This approach avoids ambiguity about image provenance and makes the transformation traceable. The analysis retains the cited units and identifies the relevant specimen orientation. Values should not be transferred directly to design without matching age, curing, geometry, test method, and production variability.

The synthesis score used for the control-priority plot is qualitative and explicitly labeled as such. It ranks variables by consistency of reported influence, potential magnitude, and feasibility of production control. It is not a fitted statistical importance measure. The figure is intended to structure a control plan and should be recalibrated using project data.

IX. RESULTS

The Le mixture series increases total binder from 537 kg/m³ in Mix 1 to 919 kg/m³ in Mix 5 while sand decreases from 1612 to 1123 kg/m³. Water rises in proportion, keeping the tabulated water-to-binder ratio close to 0.28. The progression therefore primarily changes paste volume and particle balance rather than using water addition to create flow. Mix 4 has a total listed mass of 2300 kg/m³ and binder content of 827 kg/m³. Such a high binder content supports fine-nozzle extrusion and high strength but underscores the need for lower-clinker redesign when environmental performance is a project objective.

The hardened performance reported for well-printed high-performance concrete included density near 2350 kg/m³, compressive strength of 75–102 MPa, direction-dependent flexural strength of 6–17 MPa, and interlayer tensile bond of 2.3–0.7 MPa as the printing interval increased [2]. The wide flexural and bond ranges demonstrate that excellent matrix strength does not remove process anisotropy. Poorly printed material contained more large voids than well-printed material, confirming that deposition quality can dominate the intrinsic mixture potential.

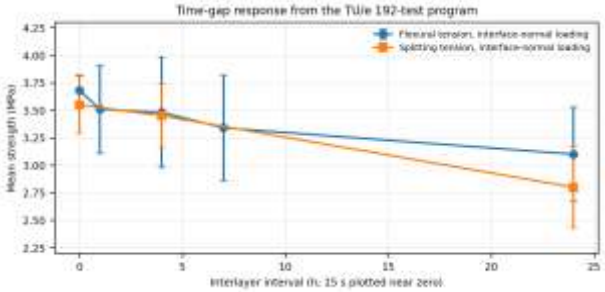


Fig. 4. Original re-plot of mean and standard deviation values reported by Wolfs et al. [5].

In the TU/e dataset, flexural tensile strength normal to the interface was 3.68 MPa at 15 s, 3.51 MPa at 1 h, 3.48 MPa at 4 h, 3.34 MPa at 7 h, and 3.10 MPa at 24 h when the waiting surface was protected. The 24 h value retained 84.2% of the 15 s reference. Splitting tensile strength was 3.55 MPa at 15 s, 3.45 MPa at 4 h, and 2.80 MPa at 24 h, retaining 78.9%. The failure path became more concentrated at the interface as delay increased [5].

Surface protection produced a larger effect than the protected time trend. At 4 h, uncovered flexural strength was 1.72 MPa compared with 3.48 MPa when covered, a 50.6% penalty. At 24 h, the reported uncovered mean was 2.28 MPa compared with 3.10 MPa covered, a 26.5% penalty. The non-monotonic uncovered means caution against fitting a simple time-only decay law to small series. They nevertheless show that dehydration can approximately halve bond-related capacity under the tested warm and dry environment.

TABLE IV. SELECTED INTERLAYER RESULTS FROM WOLFS ET AL. [5]

Condition	Mean MPa	SD MPa	Retention
Flexure III, 15 s, covered	3.68	0.14	100%
Flexure III, 4 h, covered	3.48	0.50	94.6%
Flexure III, 24 h, covered	3.10	0.43	84.2%
Splitting III, 15 s, covered	3.55	0.26	100%
Splitting III, 24 h, covered	2.80	0.37	78.9%
Flexure III, 4 h, uncovered	1.72	0.26	46.7%

At the 15 s interval, flexural strengths in loading directions I, II, and III were 4.29, 4.70, and 3.68 MPa, respectively. Compression was 28.51 MPa in direction I and 29.19 MPa in the combined II/III series, while the cast reference was 42.30 MPa. Short-interval tensile anisotropy was limited for this material-machine combination, whereas compression was about 31% lower than cast specimens. This outcome cannot be generalized to systems with different voids, fibers, bead geometry, or curing.

Nozzle height produced no clear monotonic bond trend in the cited study. This is important for control strategy: stand-off should be constrained for geometry and contact, but a universal strength correction should not be assumed. The absence of a clear effect in one robust mortar does not prove irrelevance; it shows that factor effects are conditional and may be masked within the tested range. A qualification design should therefore include interactions rather than changing one parameter at a time only.

© Author(s). This work is peer-reviewed, openly published, and permanently archived
This article is openly accessible and reusable with proper attribution.

International Journal of Science, Strategic Management and Technology
Volume **02** Issue **11** November-2026 | ISSN: **3108-1762 (Online)** | Impact Factor: 3.8
An International, Peer-Reviewed, Open Access Scholarly Journal Indexed in recognized academic databases

X. INTEGRATED DISCUSSION

The data support a state-based interpretation of interface quality. At short intervals, the earlier layer remains moist and deformable enough for the incoming bead to create intimate contact. During rest, static yield stress rises and evaporation lowers surface water. If the surface is protected, hydration-driven build-up may occur without severe moisture loss, explaining the moderate 16–21% strength reduction after 24 h in the TU/e data. If exposed, the surface can become a dry boundary and the loss can be much larger.

This interpretation reconciles apparently inconsistent literature. A time gap measured in minutes or hours cannot be compared without mixture setting behavior, temperature, humidity, wind, surface-to-volume ratio, and protection. The same principle applies to print speed and nozzle height: their effect operates through shear history, deposition pressure, geometry, and interface state. Publications and project records should therefore report the material-process-environment tuple rather than a single factor.

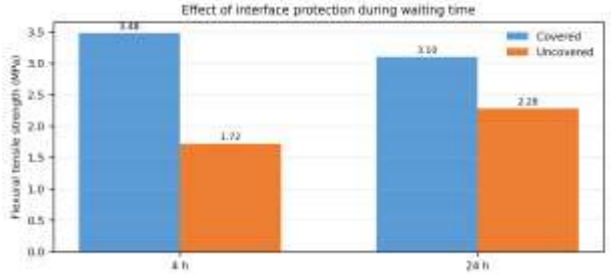


Fig. 5. Original comparison of covered and uncovered interface results reported by Wolfs et al. [5].

Mix design should be optimized against a vector of responses. Increasing fine reactive powder may improve cohesion and early strength but increase carbon intensity and shrinkage. Increasing superplasticizer may reduce pressure while delaying recovery. Accelerator improves buildability after dosing but shortens cleanout time and can create variable hydration if mixing is incomplete. Fibers improve crack resistance but orient with flow and can destabilize pumping. Multi-objective optimization is appropriate, but the objective functions must use measured, machine-relevant responses.

A practical printable window can be expressed by lower and upper bounds. Pump pressure must remain below equipment and segregation limits; static yield stress at deposition must exceed the shape-retention minimum but remain below the interface-remobilization maximum; structural build-up must support the planned load sequence; bead geometry must fall within tolerance; and bond efficiency must exceed the structural requirement. The feasible region shrinks as uncertainty grows. Production capability data should therefore be used to set operating targets away from the boundary.

The strongest implication is that printability and bond cannot be qualified independently. A mixture tuned solely for tall-stack buildability may age too fast at the interface. A mixture tuned for wet bonding may deform under rapid construction. Toolpath, layer cycle, surface protection, and staged admixture dosing provide additional control degrees of freedom. The optimum is a coordinated material and process design.

XI. PROPOSED MIX DESIGN AND QUALIFICATION PROTOCOL

Step 1 defines functional requirements: member geometry, minimum passage, nozzle, hose length, target layer dimensions, contour time, maximum interruption, build height, environmental envelope, reinforcement strategy, curing, and structural design values. Step 2 characterizes raw materials, including particle-size distribution, density, moisture, cement and supplementary material chemistry, fiber geometry, and admixture compatibility. Sand moisture is measured frequently because small water errors are large relative to the low water-to-binder ratio.

Step 3 selects aggregate grading and paste volume using packing tests or a validated model. A conservative maximum particle-to-minimum-passage ratio is established through blockage trials. Step 4 screens water-to-binder ratio and superplasticizer dosage for required dynamic flow while preventing bleeding. Filler, silica fume, viscosity modifier, or clay is adjusted to restore cohesion and recovery. Retarder is tuned to batch and hose residence; accelerator, if used, is qualified at the actual injection and mixing location.

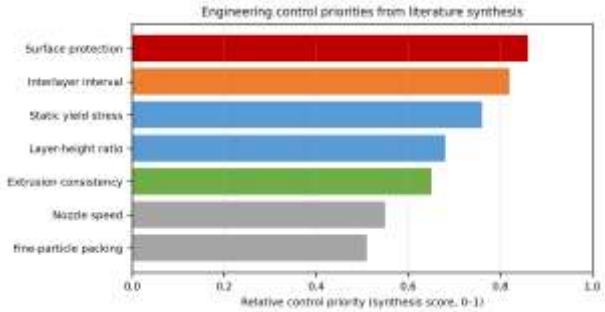


Fig. 6. Qualitative control-priority synthesis; scores structure a project control plan and are not fitted statistical coefficients.

Step 5 measures rheological evolution with a documented pre-shear and rest protocol. Static and dynamic yield indicators, plastic viscosity, and build-up are recorded at relevant temperatures. Step 6 uses a full delivery loop to map pressure against flow and time. Discharge samples are checked for grading, density, and consistency to detect filtration or segregation through the hose.

Step 7 prints single beads over straight paths, accelerations, corners, and starts/stops. Mass per length, width, height, edge quality, and command tracking are recorded. Step 8 prints representative wall segments using the slowest and fastest expected return times. Vertical deformation, lean, local buckling, overhang accuracy, and interlayer contact are measured. At least one geometry should reproduce the project's critical unsupported height or curvature.

Step 9 tests interfaces at minimum, nominal, maximum, and interruption time gaps; environmental extremes; and treated or protected conditions. Direct or splitting tension and shear are selected based on structural demand, with matched matrix controls. Step 10 tests hardened compression, flexure, shrinkage, absorption or transport, and durability in relevant orientations. Statistical characteristic values are developed from production-representative samples.

TABLE V. STAGED QUALIFICATION GATES

Gate	Evidence required	Decision
Materials	Grading, moisture, compatibility	Proceed or reformulate
Delivery	Stable pressure and discharge	Qualify pump-hose range
Deposition	Continuous accurate bead	Set Q/v and stand-off

© Author(s). This work is peer-reviewed, openly published, and permanently archived
This article is openly accessible and reusable with proper attribution.

International Journal of Science, Strategic Management and Technology
Volume 02 Issue 11 November-2026 | ISSN: 3108-1762 (Online) | Impact Factor: 3.8
An International, Peer-Reviewed, Open Access Scholarly Journal Indexed in recognized academic databases

Gate	Evidence required	Decision
Build	Stable critical geometry	Set layer-cycle window
Interface	Bond efficiency and failure mode	Set gap/protection rule
Hardened	Directional strength and durability	Structural acceptance

Step 11 establishes a process specification: constituent tolerances, allowable temperature and moisture, mixer energy and time, pump-pressure envelope, flow-to-speed ratio, nozzle stand-off, geometric tolerances, maximum unprotected gap, protection procedure, sensor alarms, sampling frequency, and disposition of nonconforming material. Changes are categorized by risk so that minor adjustments require verification while major changes trigger requalification.

XII. PRODUCTION MONITORING AND CLOSED LOOP CONTROL

The minimum production record links every bead segment to batch, time, toolpath, commanded and measured speed, pump command, pressure, nozzle position, ambient conditions, and interruptions. A synchronized clock is essential. Without temporal alignment, a later defect cannot be traced to pressure fluctuation, acceleration, or excessive layer interval. Data should be stored at a rate sufficient to detect the shortest relevant process event.

Flow can be estimated from pump displacement and calibrated against mass or volume. Pressure sensors placed near the pump and print head distinguish line losses from nozzle restriction. A rising pressure at constant flow may indicate structural build-up, temperature change, blockage, or filtration. A falling pressure with widening beads may indicate excess water or admixture. Alarm logic should use rate-of-change and persistence to avoid both missed drift and nuisance stops.

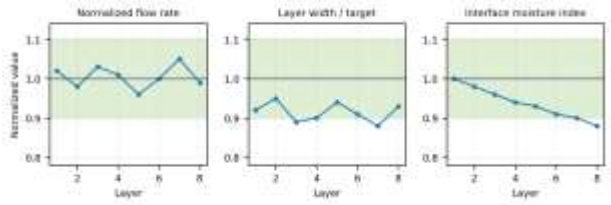


Fig. 7. Example normalized production dashboard illustrating simultaneous control of delivery, geometry, and interface state.

Geometric sensing can use line lasers, cameras, or depth sensors to compare the as-printed bead with the digital path. The controller can adjust pump command or travel speed within qualified bounds. Geometry correction cannot compensate for every material fault; a bead may have correct width but poor internal contact. Surface imagery, thermal response, moisture proxies, and occasional destructive or non-destructive tests are needed to connect appearance with interface quality.

Interruption management is a preplanned state machine. A short pause may require maintaining cover and resuming within the qualified time. A longer pause may require surface assessment and approved treatment. Beyond a limit, the layer is treated as a construction joint with a separate procedure or the print is rejected. The operator should not improvise misting, brushing, or admixture changes without a qualified instruction.

Control charts should be maintained for normalized flow, layer width, height, pressure, temperature, and interface indicators. Limits are based on process capability and engineering acceptance, not merely historical mean ±3 standard deviations. A stable but biased process can still be nonconforming. Trend rules identify gradual hose build-up or changing sand moisture before a hard limit is crossed.

TABLE VI. PRODUCTION CONTROL AND RESPONSE LOGIC

Signal	Action limit example	Immediate response
Pump pressure	Outside qualified envelope	Pause and inspect delivery
Flow/speed ratio	Sustained area error	Correct within bounded range
Layer width	Local minimum or trend	Mark segment and correct
Interlayer interval	Exceeds protected limit	Apply interruption procedure
Surface condition	Outside qualified band	Treat, joint, or reject
Ambient state	Outside envelope	Enclose, condition, or stop

Human oversight remains necessary. Automation changes the role from manual placement to system supervision, material verification, exception handling, and safety. Training should cover rheology, equipment hazards, digital files, sensor reliability, cleaning windows, and structural consequences of process deviations. A stop decision must be protected from schedule pressure by clear authority and traceable criteria.

XIII. STRUCTURAL DESIGN IMPLICATIONS

Structural models should distinguish material directions associated with the print path, layer plane, and build direction. Orthotropic or layered properties may be required for tension, shear, fracture, and transport, even when compressive anisotropy is limited. The weakest credible interface orientation should govern members subjected to transverse tension or shear. Printed texture, voids, openings, and reinforcement discontinuities must be included in the load path.

Characteristic values should be derived from production-representative populations. Coupon specimens printed in short laboratory walls may have shorter return times and better environmental control than a full building. A qualification wall should reproduce critical contour length, height, starts/stops, and curing. Samples extracted from the member or a simultaneously printed witness element preserve process history better than separately cast cubes.

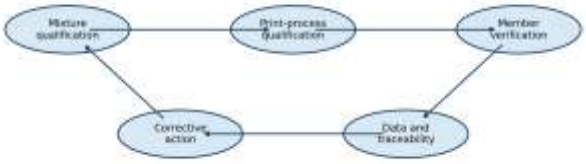


Fig. 8. Closed quality loop linking qualification, production, verification, traceability, and corrective action.

Bond strength is not the only interface property. Fracture energy controls crack propagation, while permeability and sorptivity affect durability. Repeated thermal or moisture cycling may exploit connected interface pores. Reinforcement crossing layers changes shear transfer and crack control, but insertion methods can disturb fresh geometry. Structural design and production planning must be coordinated early.

Geometric tolerance affects structural capacity. Wall thickness, local necking, path deviation, and voids change area and eccentricity. A digital twin should use verified as-built geometry where deviations are material. Acceptance may combine global tolerances with local minimum thickness and defect rules. Corrective machining or filling must use compatible materials and documented structural evaluation.

© Author(s). This work is peer-reviewed, openly published, and permanently archived
This article is openly accessible and reusable with proper attribution.

The design basis should specify the qualified material-machine combination and permitted parameter envelope. Substitution of a pump, hose, nozzle, sand source, admixture, or print sequence is not automatically equivalent. A change-control matrix should identify which verification tests are necessary. This links structural reliability to manufacturing configuration in the same manner that welded or precast systems control procedures and qualifications.

XIV. SUSTAINABILITY AND SCALE UP

Formwork elimination and geometric material efficiency are potential sustainability advantages, but they do not guarantee lower embodied carbon. Early printable mixtures often use high binder contents and fine powders. The Le Mix 4 benchmark contains 827 kg/m³ of cementitious binder, much greater than many conventional concretes. A fair assessment compares functionally equivalent members and includes cement content, reinforcement, waste, formwork, energy, transport, curing, and service life [3], [4].

Lower-clinker printable mixtures can use slag, fly ash, calcined clay, limestone, recycled fines, or alternative binders, but variability and early-age response require attention. Supplementary materials may improve pumping while slowing build-up, or change admixture demand with temperature. Sustainability optimization must retain print reliability; aborted prints and weak interfaces erase material savings.

Coarser aggregate reduces paste demand but challenges hoses and nozzles. Graded aggregate, larger passages, and controlled pumping can move 3D concrete printing from mortar toward true concrete. The printer scale should not be increased without recalculating pressure, bead self-weight, return time, heat, and stability. A larger wall contour can lengthen the interval even when travel speed is unchanged.

Modular off-site printing offers controlled environment and quality, while on-site printing reduces transport of large elements. The choice changes curing, tolerances, joints, lifting, and logistics. Hybrid systems may print stay-in-place shells and place conventional concrete or reinforcement. Such systems should evaluate the bond between printed and cast materials and avoid assuming monolithic action.

Life-cycle claims require durability data in the printed directions. Interfaces can create preferential fluid transport, while optimized geometry can reduce exposure or enable replaceable components. Service-life modeling should incorporate measured anisotropic transport and crack behavior. End-of-life planning should consider reinforcement, composite layers, and separation, not only material mass saved during fabrication.

XV. LIMITATIONS AND FUTURE RESEARCH

The secondary analysis is limited by published aggregate statistics. Raw observations were unavailable for all series, preventing consistent hypothesis tests, interaction models, or uncertainty propagation. The two principal datasets use different materials, machines, ages, and tests; they are interpreted comparatively but not pooled into a universal predictive equation. The proposed acceptance ranges are therefore procedural examples, not code values.

Test standardization remains a priority. Specimen geometry, interface count, extraction, loading direction, age, curing, and failure classification vary across studies. Round-robin programs should quantify repeatability and reproducibility of fresh-state, buildability, and bond tests. Reference materials and shared digital toolpaths would help separate laboratory method effects from material effects.

Research should connect in-process signals to structural performance. Pressure, motor current, geometry, moisture, acoustic response, and thermal imaging can be fused into probabilistic defect indicators. Models require deliberately varied, well-documented prints with destructive ground truth. Generalization across machines should be tested rather than assumed.

Mixture design research should reduce clinker and paste while increasing aggregate size, maintaining robust pumping and interface quality. Staged dosing, reversible thixotropy, internal curing, and surface-conditioning methods deserve factorial experiments. Optimization objectives should include carbon, cost, pressure, dimensional error, build height, bond efficiency, shrinkage, and durability.

Full-scale structural demonstrations need transparent production records and long-term monitoring. Small coupons do not reproduce contour times, reinforcement operations, interruptions, weather, or restraint in buildings. Performance-based standards can develop from linked databases that retain material certificates, machine configuration, sensor streams, specimen results, and member outcomes.

XVI. CONCLUSIONS

This paper establishes that printability is a coupled material-machine-time property. Pumpability, extrudability, buildability, open time, geometry, and bond must be evaluated together under production-representative shear and environmental histories. A mixture that passes one test is not necessarily printable for a given structure.

Published data show the structural importance of interface condition. In the analyzed TU/e program, protected flexural tensile strength decreased from 3.68 MPa at 15 s to 3.10 MPa at 24 h, while protected splitting tensile strength decreased from 3.55 to 2.80 MPa. Leaving the 4 h interface uncovered reduced flexural strength from 3.48 to 1.72 MPa. Thus, time-gap control without moisture-state control is inadequate.

The historical high-performance mix series demonstrates how paste volume and particle balance can be increased while holding water-to-binder ratio near 0.28. It also highlights a sustainability challenge: successful early mixtures contain high binder contents. Future optimization must reduce clinker and paste without sacrificing pumping stability, recovery, or bond.

Qualification should approve the complete configuration: materials, batching, mixer, pump, hose, nozzle, toolpath, layer cycle, environment, protection, curing, and tests. Production monitoring should link pressure, flow, speed, geometry, and interface state to every printed segment. Interruption rules and change control are essential structural controls.

Reliable automated concrete construction will emerge from manufacturing discipline rather than a universal printable recipe. Traceable data, standardized tests, conservative process windows, and feedback control can convert an intrinsically time-dependent material into a repeatable construction system.

© Author(s). This work is peer-reviewed, openly published, and permanently archived
This article is openly accessible and reusable with proper attribution.

APPENDIX A. GOVERNING INDICATORS

The following compact indicators support calculation sheets and digital quality records. Symbols and test procedures must be defined in the project specification; the equations do not replace calibration or structural verification.

(1)

Bingham approximation for yielded flow, where τ_0 is dynamic yield stress, μ_p is plastic viscosity, and $\dot{\gamma}$ is shear rate.

Early-age linear structural build-up approximation over a validated rest interval.

$$Q = k_s b h v \quad (3)$$

Volumetric delivery relation using bead shape factor k_s, measured width b, height h, and nozzle speed v.

$$\eta_b = f_{interface} / f_{matrix}$$

Bond-efficiency ratio using matched test method, age, orientation, and curing.

$$R_{24h} = 100 f_{24h} / f_{15s}$$

Strength retention used in the secondary analysis relative to the short-interval reference.

APPENDIX B. RECOMMENDED REPORTING CHECKLIST

TABLE VII. MINIMUM REPRODUCIBILITY INFORMATION

Category	Minimum reported fields
Materials	Sources, chemistry, grading, moisture, masses, admixture solids, fiber geometry
Fresh state	Temperature, density, test geometry, pre-shear, rest, yield/flow indicators
Equipment	Mixer, pump, hose length/diameter, nozzle geometry, sensor calibration
Toolpath	Speed, acceleration, layer size, contour time, starts/stops, stand-off
Environment	Air/material/substrate temperature, RH, wind, sun, protection
Specimens	Extraction, dimensions, interface count, orientation, curing, age, rate
Statistics	n, individual values or repository, mean, SD, failures, exclusions
Traceability	Batch, timestamps, configuration, deviations, corrective actions

REFERENCES

[1] T. T. Le, S. A. Austin, S. Lim, R. A. Buswell, A. G. F. Gibb, and T. Thorpe, “Mix design and fresh properties for high-performance printing concrete,” Materials and Structures, vol. 45, pp. 1221–1232, 2012, doi: 10.1617/s11527-012-9828-z.

[2] T. T. Le, S. A. Austin, S. Lim, R. A. Buswell, R. Law, A. G. F. Gibb, and T. Thorpe, “Hardened properties of high-performance printing concrete,” Cement and Concrete Research, vol. 42, no. 3, pp. 558–566, 2012, doi: 10.1016/j.cemconres.2011.12.003.

[3] R. A. Buswell, W. R. Leal de Silva, S. Z. Jones, and J. Dirrenberger, “3D printing using concrete extrusion: A roadmap for research,” Cement and Concrete Research, vol. 112, pp. 37–49, 2018, doi: 10.1016/j.cemconres.2018.05.006.

[4] T. Wangler et al., “Digital concrete: A review,” Cement and Concrete Research, vol. 123, art. 105780, 2019, doi: 10.1016/j.cemconres.2019.105780.

[5] R. J. M. Wolfs, F. P. Bos, and T. A. M. Salet, “Hardened properties of 3D printed concrete: The influence of process parameters on interlayer adhesion,” Cement and Concrete Research, vol. 119, pp. 132–140, 2019, doi: 10.1016/j.cemconres.2019.02.017.

[6] Y. W. D. Tay, G. H. A. Ting, Y. Qian, B. Panda, L. He, and M. J. Tan, “Time gap effect on bond strength of 3D-printed concrete,” Virtual and Physical Prototyping, vol. 14, no. 1, pp. 104–113, 2019, doi: 10.1080/17452759.2018.1500420.

[7] B. Panda, S. C. Paul, N. A. N. Mohamed, Y. W. D. Tay, and M. J. Tan, “Measurement of tensile bond strength of 3D printed geopolymer mortar,” Measurement, vol. 113, pp. 108–116, 2018, doi: 10.1016/j.measurement.2017.08.051.

$$\tau_0(t) = \tau_{0,initial} + A_{thix} t \quad (4)$$

[8] V. N. Nerella, M. Krause, and V. Mechtcherine, “Direct printing test for buildability of 3D-printable concrete considering economic viability,” Automation in Construction, vol. 109, art. 102986, 2020.

[9] T. Marchment and J. G. Sanjayan, “Mesh reinforcing method for 3D concrete printing,” Automation in Construction, vol. 109, art. 102992, 2020.

(5)

[10] M. Moini, J. Olek, B. A. Magee, P. D. Zavattieri, and J. P. Youngblood, “Additive manufacturing and characterization of architectured cement-based materials via X-ray micro-computed tomography,” Additive Manufacturing, vol. 24, pp. 96–108, 2018, doi: 10.1016/j.addma.2018.08.003.

[11] V. N. Nerella, S. Hempel, and V. Mechtcherine, “Effects of layer-interface properties on mechanical performance of concrete elements produced by extrusion-based 3D-printing,” Construction and Building Materials, vol. 205, pp. 586–601, 2019, doi: 10.1016/j.conbuildmat.2019.01.235.

[12] A. Perrot, D. Rangeard, and A. Pierre, “Structural built-up of cement-based materials used for 3D-printing extrusion techniques,” Materials and Structures, vol. 49, pp. 1213–1220, 2016, doi: 10.1617/s11527-015-0571-0.

[13] N. Roussel, “A thixotropic model for fresh fluid concretes: Theory, validation and applications,” Cement and Concrete Research, vol. 36, no. 10, pp. 1797–1806, 2006, doi: 10.1016/j.cemconres.2006.05.001.

[14] G. De Schutter et al., “Vision of 3D printing with concrete—Technical, economic and environmental potentials,” Cement and Concrete Research, vol. 112, pp. 25–36, 2018, doi: 10.1016/j.cemconres.2018.06.001.

[15] V. Mechtcherine et al., “Extrusion-based additive manufacturing with cement-based materials—Production steps, processes, and their underlying physics: A review,” Cement and Concrete Research, vol. 132, art. 106037, 2020, doi: 10.1016/j.cemconres.2020.106037.

[16] F. P. Bos, R. J. M. Wolfs, Z. Y. Ahmed, and T. A. M. Salet, “Additive manufacturing of concrete in construction: Potentials and challenges of 3D concrete printing,” Virtual and Physical Prototyping, vol. 11, no. 3, pp. 209–225, 2016, doi: 10.1080/17452759.2016.1209867.

[17] S. Lim, R. A. Buswell, T. T. Le, S. A. Austin, A. G. F. Gibb, and T. Thorpe, “Developments in construction-scale additive manufacturing processes,” Automation in Construction, vol. 21, pp. 262–268, 2012, doi: 10.1016/j.autcon.2011.06.010.

[18] A. J. Babafemi, C. Kolawole, M. M. Paul, and B. Panda, “A concise review on interlayer bond strength in 3D concrete printing,” Sustainability, vol. 13, no. 13, art. 7137, 2021, doi: 10.3390/su13137137.

[19] I. Hager, A. Golonka, and R. Putanowicz, “Interlayer bond strength testing in 3D-printed mineral materials for

© Author(s). This work is peer-reviewed, openly published, and permanently archived
This article is openly accessible and reusable with proper attribution.

construction applications," Materials, vol. 15, art. 4112, 2022, doi: 10.3390/ma15124112.
[20] A. U. Rehman and J. H. Kim, "3D concrete printing: A systematic review of rheology, mix designs, mechanical, microstructural, and durability characteristics," Materials, vol. 14, art. 3800, 2021, doi: 10.3390/ma14143800.

© Author(s). This work is peer-reviewed, openly published, and permanently archived
This article is openly accessible and reusable with proper attribution.